Exothermic Reaction Kinetics in High Energy Density Al-Ni with Nanoscale Multilayers Synthesized by Cryomilling

Minseok Oh [1], Min Chul Oh [1], Deokhyun Han [1,2], Sang-Hyun Jung [3] and Byungmin Ahn [1,4,*] (ID)

[1] Department of Energy Systems Research, Ajou University, Suwon 16499, Korea; main4382@ajou.ac.kr (M.O.); minlovehyo@ajou.ac.kr (M.C.O.); hankani@iae.re.kr (D.H.)
[2] Advanced Materials & Processing Center, Institute for Advanced Engineering, Yongin 17180, Korea
[3] The 4th Research and Development, Agency for Defense Development, Daejeon 34060, Korea; sanghyun@add.re.kr
[4] Department of Materials Science and Engineering, Ajou University, Suwon 16499, Korea
* Correspondence: byungmin@ajou.ac.kr; Tel.: +82-31-219-3531; Fax: +82-31-219-1613

Abstract: The Al-Ni system is known as a high energy density materials (HEDM) because of its highly exothermic nature during intermetallic compound (IMC) formation. In this study, elemental Al and Ni powder were milled to explore the effect of cryomilling atmosphere on the microstructure and exothermic behavior. Scanning electron microscope (SEM) observations show continuous structural refinement up to 8 h of cryomilling. No IMC phase was detected in the X-ray diffraction (XRD) spectrum. Differential thermal analyzer (DTA) results show two exothermic peaks for 8 h cryomilled powder as compared to that of powder milled for 1 h. The ignition temperature of prepared powder mixture also decreased due to gradual structural refinement. The activation energy was also calculated and correlated with the DTA and SEM results. The cryomilled Al-Ni powder is composed of fine Al-Ni metastable junctions which improve the reactivity at a lower exothermic reaction temperature.

Keywords: high energy density materials; Al-Ni; cryomilling; exothermic reaction; activation energy

1. Introduction

High energy density materials (HEDM) are a class of energetic materials that react when exposed to extreme conditions such as high temperature, electric shock, or physical impact, releasing a lot of chemical energy as heat [1–3]. Due to these reactive properties, HEDMs are widely used in the fields where an enormous amount of energy needs to be emitted in a short period of time. They are applied to explosives, propellants, fossil fuels, and thermite materials [3–5]. The metal + metal bonded HEDMs are also referred to as solid flame materials or gasless exothermic materials. The most popular reactive material system is Al-Ni [1–5]. In the Al-Ni system, when intermetallic compounds (IMC) are formed, a large amount of heat reaching 59.53 kJ/mol can be generated. Similarly, when Al-Ni mixture forms a certain microstructure, Al-Ni bulk mixture can be reacted and exploded which make this material applicable to various energetic fields [6,7]. However, the Al-Ni system has its limitations as utilizing the energy of impact because of its ambiguous reactivity. The thermodynamic modification is therefore necessary to improve its usability and reliability. Several reactive Al-Ni systems have been produced by methods like combustion synthesis [8], mixing and pressing of powders [9,10], welding [11,12], forging [13], rolling [14,15], vacuum deposition [11,15], cladding [16], and high energy ball milling [17–19]. It is well-known fact that the reactivity of these composites depends strongly on their corresponding microstructures. Among various methods as mentioned above, most commonly used approach is to refine the Al and Ni powder particles to nano-size, and increase the contact area

of Al and Ni particles to accelerate the reaction kinetics considerably. High-energy ball milling at room temperature is the most popular one to prepare Al-Ni composites [17–19]. However, despite of the high reactivity, nano-sized pure Al is hazardous to handle at room temperature. This exothermic tendency is particularly sensitive to Al, as the disruption of the inherent Al_2O_3 layer causes its vigorous reaction oxygen at the atmosphere. Moreover, the local temperature increase in milling process creates Al-Ni IMCs more readily and affects the interface shape and milling efficiency. Therefore, in order to control the reactivity of Al to concentration on the reaction with Ni, it is necessary to reduce the exposed surface of pure Al to the surrounding atmosphere for avoiding oxidation. Therefore, in this work, the authors have attempted to prepare Al-Ni composite powder by cryomilling technique which can suppress the extra local heat generated during the milling. Cryomilling, can thus avoid the crystal recovery and maximize the shear stress suggesting a better and unique microstructure [20]. There were a limited information on the effect of milling at cryogenic temperatures ($<-160\ °C$) on microstructure and reactivity of the Al-Ni system [21]. Especially at low temperatures, in addition to fine particle size, the cryogenic atmosphere could suppress the extent of reaction of Al-Ni resulting in a more reactive material controlling the Al-Ni reaction temperature. This is a great advantage of cryomilling when compared with the high energy ball milling.

In this study, the effect of cryomilling on the microstructure, reactivity of Al-Ni alloy prepared from elemental Al and Ni powder mixtures. The effect of structure on thermal properties was investigated by differential thermal analysis, and the reaction kinetics was studied by calculating activation energy of the Al-Ni reaction through Kissinger analysis.

2. Experimental Procedures

2.1. Materials and Processes

The Ni powder in this experiment, was prepared by a bottom-up method with an average size of 4.5 μm. Additionally, Al powder was gas atomized powder with an average size of 6 μm. For the cryomilling process, Al and Ni powder were mixed in a molar ratio of 50:50, resulting in the final composition of Ni 68 wt. % and Al 32 wt. %. The powder mixture was put into a 1 L stainless steel vessel having stainless steel balls (diameter 4.35 mm) for attrition milling. The milling temperature was set at $-160 \pm 5\ °C$ by flowing the liquid nitrogen around the vials for 8 h. The ball to powder weight ratio was 30:1 and the impeller rotation speed was 180 rpm. To control the lubrication and coarsening of the powder, 2 wt. % of stearic acid powder as a process control agent (PCA) was also added in the powder mixture.

2.2. Characterization

The phase evolution of the Al-Ni powder mixture after cryomilling was analyzed by a tabletop X-ray diffraction (XRD) instruments (Miniflex2, Rigaku, Tokyo, Japan) operating at 30 mA and 15 kV with a Cu target (wavelength is 0.154 nm). The surface morphology and the cold-welding behavior of powder particles were examined in a field emission scanning electron microscope (FE-SEM) (JSM-6700F, JEOL, Tokyo, Japan) operating at 20 kV. For analyzing alloying behavior, the backscattered electron (BSE) detector was used in this research. The sample preparation was accomplished by cold mounting, grinding, and polishing up to 1 μm diamond paste following standard metallographic procedures. The compositional analysis of the samples was estimated by energy-dispersive spectroscopy (EDS) techniques. The cryomilled powder mixtures were analyzed using a differential thermal analyzer (DTA) (STZ 409PC, Netzsch, Selb, Germany). The samples were annealed in alumina pans from 400 to 800 °C at a heating rate of 10 °C/min under an argon atmosphere. The onset reaction temperature was observed, and the activation energy of the reaction was calculated following the Kissinger method [22]. In order to minimize the effect of particle shape and size, the material was molded into a circular specimen having a thickness and diameter of 50 mm at a load of seven tons (to have 85% relative density after molding).

3. Results and Discussion

3.1. Surface Morphology

The evolution of the surface morphology of Al-Ni powder as a function of cryomilling time is shown in Figure 1. The shape of the as-received powder (Al and Ni, before milling) is shown in Figure 1a. The as-received Ni powder has a polyhedral shape while the as-received Al powder is of spherical shape. Figure 1b–d show how the size and shape of these powders vary with milling time. Using a BSE detector in SEM, the heavier elements appear brighter in micrograph, because higher atomic number elements backscatter electrons more strongly than lower atomic number elements. Thus, in the BSE micrographs in this study, the Al-rich phase appears darker, and the Ni-rich phase appears brighter. It can be seen that at the first stage of cryomilling (1 h), the average powder particle size increases from 10 to 20 μm as compared to that of as-received powder particles (Ni < 5 μm and Al < 10 μm) in Figure 1a,b. This shows that cold-welding of powder particles dominates over the powder fracturing. The powder morphology is plate-shaped as shown in Figure 1b due to the plastic deformation of Al and Ni powder. This trend continues up to 4 h of cryomilling as shown in Figure 1c. The darker Al particles were stuck on the brighter Ni ones and piled up, as shown in a red circle in Figure 1c. The morphology drastically changes after 8 h of cryomilling in Figure 1d. The fraction of plate-shaped particles was reduced, and particles became noticeably irregular. It means the Al and Ni powder mixture is work hardened and the effects of cold-welding and fracturing on the morphology become balanced [23,24]. In other words, with increasing milling time, the particle size distribution was narrowed down. It is also noticed that the plate-shaped Al particles were combined, and Ni particles were stuck together on the Al plates. However, in the particle shape analysis, it is not clear that the bonding between Al-Ni and cold-welding certainly occurred. Finally, after 8 h of cryomilling as shown in Figure 1d, most of the powders have both brighter Ni particles and darker Al particles with unclear boundaries as shown in the encircled regions in Figure 1d.
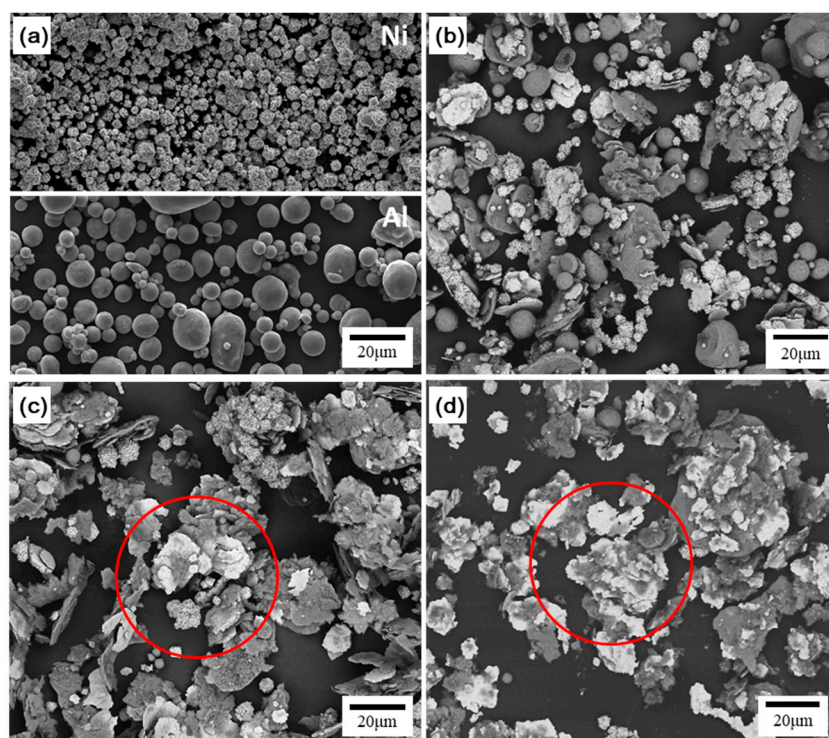

Figure 1. SEM (scanning electron microscope) and BSE (backscattered electron) micrographs showing the morphology of cryomilled Al-Ni powder for different milling times (darker is Al, brighter is Ni): (**a**) 0 h; (**b**) 1 h; (**c**) 4 h; and (**d**) 8 h.

As discussed earlier from the earlier SEM observations, although the multilayered Al-Ni structure is not clear yet, the structural refinement is maximized after 8 h of cryomilling. This microstructural evolution is also observed in the powders processed by other high energy milling techniques even in 20 min milling without any PCA. It is inferred that the energy of cryomilling is lower than that of high energy milling, and that the surface energy between powder particles is minimized due to PCA. This indicates that cryomilling induces a homogeneous alloying of Al and Ni powder and there are no other interfaces observed as compared to room temperature ball milling where heterogeneous alloying predominates.

3.2. Microstructural Evolution

Figure 2 shows the cross-sectional microstructure of 1 h and 8 h cryomilled powders. The cold-welded contacts between Al and Ni powders are observed after 1 h milling indicated by yellow arrows in Figure 2a. It can be seen that most of the Al and Ni powders are cold-welded, while some of Al-Al and Ni-Ni powder particles were segregated and clustered together. At this stage, it can be considered that there is no significant difference in the thermodynamic behavior of the Al-Ni powder mixture due to the increase of contact area between Al and Ni. On the other hand, in 8 h cryomilled powder shown in Figure 2b, smaller size particles were observed compared to the 1 h cryomilling. The powder shape is changed into a plate-like structure compared with 1 h. The size of Al and Ni powders are decreased with increased milling time. In particular, as expected from the powder morphology in Figure 1, a layered structure of Al-Ni mixture is confirmed where bonded Al and Ni structure is repeated two or three times to form 6–8 layers in Figure 2b. The most characteristic feature of repeated layers is shown by the red circles in at a high resolution in Figure 2c after 8 h of milling. The particle size difference, number of bonded Al-Ni structures, and frequency of the repetitive layer after 1 and 8 h milling were also examined. It can be seen that cold-welding dominates during the 1 h milling while fracturing phase is predominant during 8 h of milling time. The cold-welding of the particles was confirmed from the blurring of the boundaries of the bonded regions in Al-Ni plates. As a result, it is confirmed that most Al and Ni particles are bonded to each other in Figure 2. The repeated cold-welding of powders results in homogeneous mixing of Al and Ni powders. The driving force for the cold welding between Al and Ni powders comes from the difference in surface energy of cold welding between Al and Ni powder. The area marked in yellow is the part where this surface energy difference is overcome, and cold welding occurs. Even though the rpm or ball-to-powder weight ratio was not changed at 8 h, the cold-welding fraction of Al and Ni was increased. This is because the number of collisions between Al and Ni is increased, the surface energy is overcome, and the amount of the welded powder is increased, although the amount of energy applied to the powder during milling was not changed [23,24].

Figure 2c clearly shows the junctions of Al and Ni bonded particles. The cold-welded part is shown in red circles which is the contact surface of the brighter Ni phase and the darker Al phase. It is confirmed that the interfaces between the two phases are not clearly distinguished so that the Al and Ni phases in the red circles had diffused each other. Therefore, it is judged that there is almost no Al_2O_3 film on each joint surface generated by the milling and so on [25], and it can be concluded that the boundary between the two phases appears blurred indicating disordered metastable junctions. These metastable junctions serve as active sites for the diffusion, and IMC phases can be formed by an exothermic phase transformation [26]. However, at this stage, the energy required for this phase transformation is much lower than that required when Al and Ni particles simply contact each other without bonding. Therefore, the reaction can actively occur at these metastable junctions at lower temperatures. This exothermic reaction is not limited at the metastable junctions, but promoted near the interface areas because temperature rise activates molecular diffusion of the two elements.

EDS analysis was conducted to confirm the existence of metastable phases. Figure 3 shows the EDS line scan results of the 8 h cryomilled sample. It was observed from the EDS spectrum that the number of counts of Ni and Al is almost equal to that of an intermediate region between Al and Ni,

thus confirming that the two phases are homogeneously alloyed [26]. In general, when Al and Ni are mixed in an equal atomic ratio at room temperature, the stable phase is simply a randomly-mixed Al-Ni phase with IMCs. Since the phases are not in an equilibrium state, they can react at a high temperature to form compounds. In this case, the metastable solid solution in Figure 3b of the Al-Ni powder is activated so that the diffusion becomes easier and the reaction starts at lower temperatures (lower activation energy).
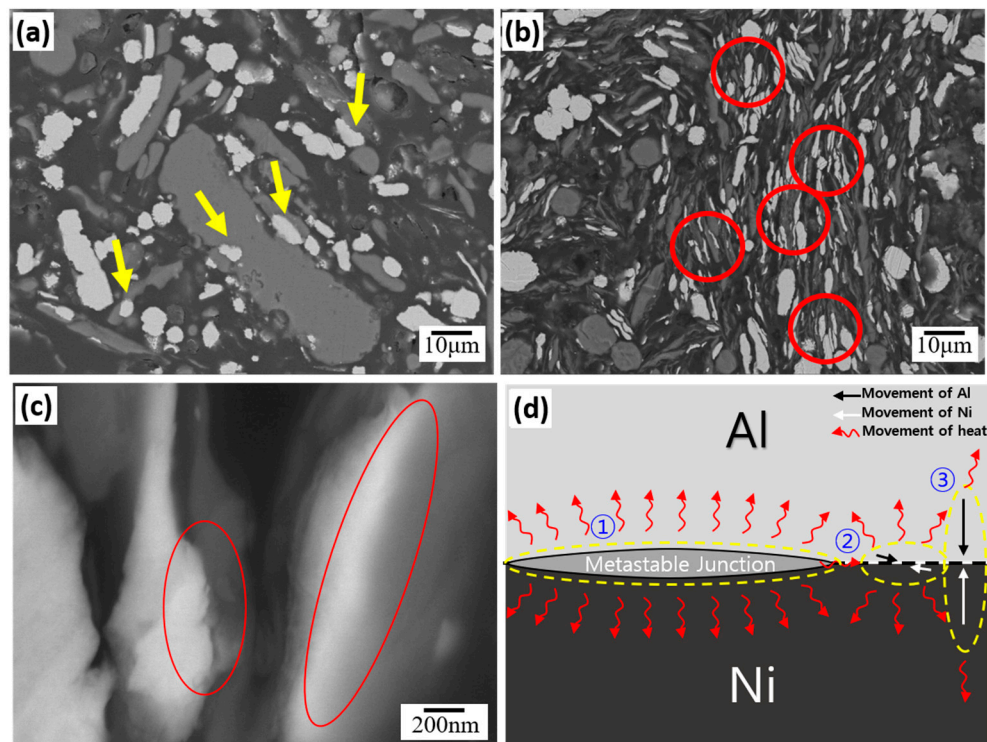

Figure 2. BSE micrographs showing the cross-sectional morphology of cryomilled powder for different milling times (darker is Al, brighter is Ni) (**a**) 1 h; (**b**) 8 h; (**c**) high-resolution image of (**b**); and (**d**) the diagram of exothermic reaction at surface of Al-Ni cryomilled mixture. ① is the reaction on the metastable junction with heat generation, and ② is the surface reaction caused by the diffusion of surface Al and Ni which is induced by generated heat of metastable junction; ③ is the bulk diffusion and reaction which is induced by the generated heat of other reactions.
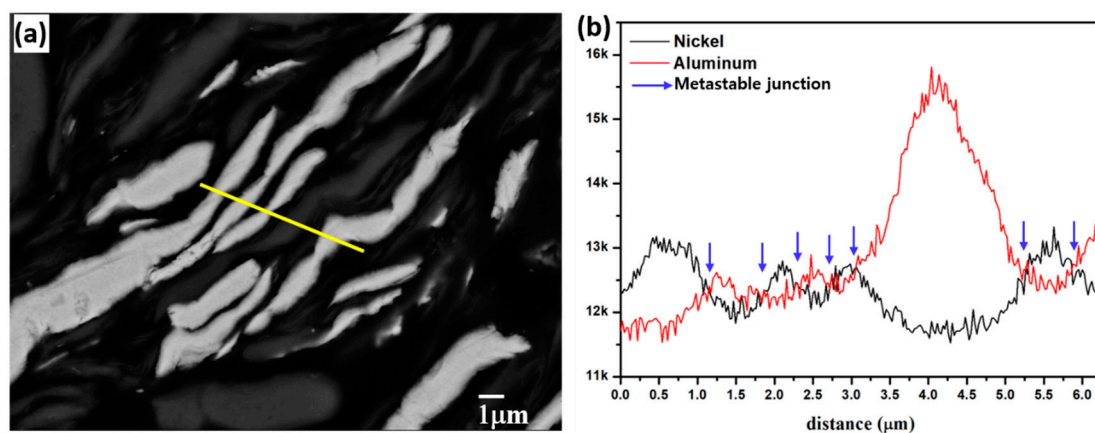

Figure 3. (**a**) BSE micrograph of 8 h cryomilled powder for EDS line scan, and (**b**) EDS line scan result of the yellow line in (**a**) showing metastable junctions of the Al-Ni mixture.

3.3. Thermal Property

Figure 4 shows DTA analysis results of the cryomilled Al-Ni powder mixture for various milling times. The change in ignition temperature with different milling times is also shown. It is seen from the Figure 4a that several exothermic reaction peaks appear for each powder mixture. The ignition temperature is also found to decrease gradually with increasing milling time in Figure 4b.
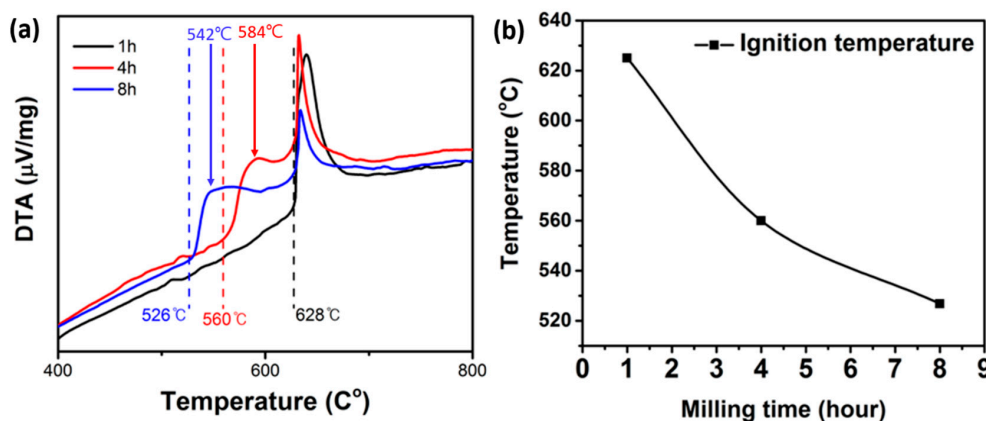

Figure 4. (**a**) DTA (differential thermal analyzer) curves of Al-Ni powder mixture cryomilled for different times (dashed temperature is first reaction starting point and arrowed temperature is heat treatment temperature for XRD data); and (**b**) the variation of ignition temperature as a function of cryomilling time.

The minimum temperature at which the two elements are intermixed with each other is ~640 °C, according to the Al-Ni phase diagram [8]. It can be seen that for 1 h sample, the exothermic reaction starts at the temperature of 628 °C and ends at 640 °C. On the other hand, two exothermic peaks appeared for the powders milled for 4 and 8 h. The starting temperature of the first reaction peak decreases as the milling time becomes longer. For example, the initial exothermic reaction takes place at 560 °C and 526 °C for 4 and 8 h milled powders, respectively (Figure 4b), followed by a second exothermic reaction at 628 °C. This can be attributed to the repeated cold-welding and fracturing of the powders causes a refinement in microstructure as shown in red circles of Figure 1c,d. The contact surface area of the Al-Ni powders increases and hence the reaction rate also increases at a faster speed. It seems that the cold-welded Al-Ni powder reacts before their eutectic temperature. Due to the difference in microstructures, the difference in the first exothermic reaction onset temperature of 1 and 8 h powders were found to be about 100 °C in Figure 4b. Additionally, a difference of about 68 °C was observed from the first exothermic reaction onset temperature of the powder milled for 1 and 4 h.

It is a noteworthy point that the thermal analysis was performed on the molded samples to minimize the effect of shape and size, therefore the porosity in the samples can be assumed to be constant since the density of the molded body is the same. In this case, the influence of the shape of the powder on the thermodynamic behavior can be minimized and the physical distance between the Al-Ni powders can be made close to zero so that the effect of the density of the powder depending on the powder shape can be eliminated. Therefore, due to the increase of the contact area between Al and Ni through cold-welding and to the activation of the new contact surfaces, the exothermic reaction temperatures were significantly different after 4 and 8 h of cryomilling, as compared to that of 1 h milling.

3.4. Phase Evolution

The XRD patterns of Al-Ni powder mixture are shown in Figure 5. It is observed that only Al (JCPDS: 01-071-3760) and Ni phases (JCPDS: 01-071-4655) were observed. There were not any noticeable AlNi or Al_3Ni_5 IMCs present in the diffraction pattern, as shown in Figure 5. It can be seen that Al peaks

get broaden and intensity is also reduced with milling time increasing. After 8 h of milling, the Al peaks starts disappearing gradually from the spectrum. In Figure 5b, the two XRD data measured at their first reaction peak. It shows, the AlNi$_3$ are produced during first exothermic reaction of the 4 and 8 h milled powder. This proves that the first peak does not involve a recrystallization reaction, but that Al-Ni is synthesized with AlNi$_3$ (JCPDS: 01-071-5883) and Al$_3$Ni$_2$ (JCPDS: 00-003-1052).
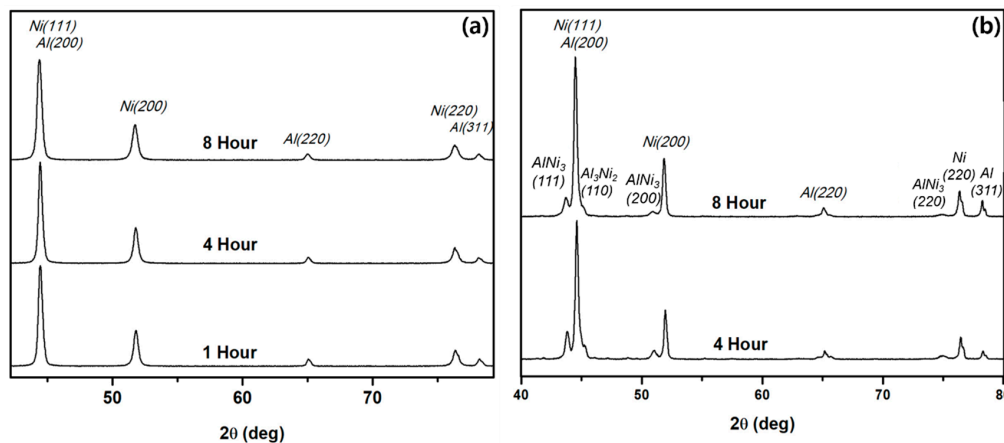

Figure 5. (**a**) XRD (X-ray diffraction) pattern of Al-Ni powder milled for different times and (**b**) XRD pattern after heat treatment at DTA first peak temperature.

If we consider the binary phase diagram of Al-Ni system in Figure 6 as given by Zhu et al. [8], it is known that six types of IMCs exist in Al-Ni system (Al$_3$Ni, Al$_3$Ni$_2$, Al$_4$Ni$_3$, AlNi, Al$_3$Ni$_5$, and AlNi$_3$). However, there is no significant trace of IMCs in the present XRD results.

Huang et al. observed the B2 AlNi phase beyond 20 h while milling in a cryogenic medium at −186 °C [27]. However, in the present work, no IMC phase is generated because the milling duration was only 8 h giving the less impact energy.
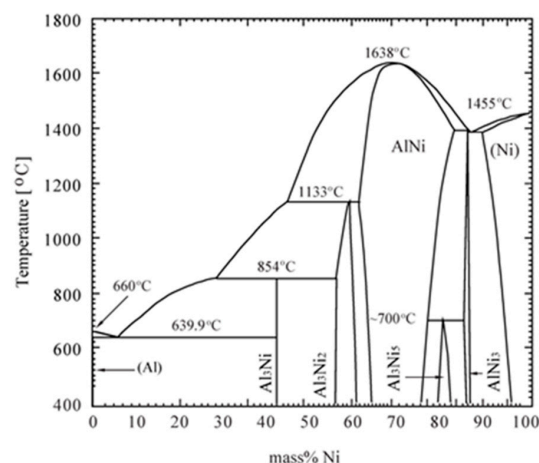

Figure 6. Binary phase diagram of Al-Ni system [8].

3.5. Activation Energy for Exothermic Reaction

In order to define the effect of cryomilling on the dynamics of the chemical reaction in the HEDM system, a thermodynamic analysis was carried out in order to calculate the activation energy. Since the cold-welded powder, with a large joint area, has a larger contact area than ordinary powder, the surface diffusion dominates the bulk diffusion and reaction proceeds very fast. In other words, Al and Ni atoms migrate mainly through the volume diffusion, however, as the milling time increases,

the surface diffusion becomes easier due to the reduction in activation energy. According to the Kissinger method [22], a solid-state reaction is represented by the following equation:

$$\frac{dx}{dt} = A(1-x)^n e^{-E_a/RT} \tag{1}$$

where $\frac{dx}{dt}$ is the velocity, A is the frequency factor, x is reacted fraction, n is empirical reaction order, E_a is activation energy, and T is absolute temperature. When the reaction is accompanied by a rise in temperature, the reaction rate $\frac{dx}{dt}$ rises to its maximum value and returns to zero when one of the reactants is depleted. This maximum occurs when the time derivative of the reaction rate is zero. Therefore, setting the result to 0 in Equation (1) gives the Kissinger equation:

$$\frac{E_a \beta}{RT_p^2} = An(1-x)e^{-E_a/RT_p} \tag{2}$$

where β is the heating rate, $\beta = \left(\frac{dT}{dt}\right)$, and T_p is the temperature at which the velocity is maximum. Simplifying the Equation (2) above:

$$-\ln\left(\frac{\beta}{T_p^2}\right) = -\left(\frac{AR}{E_a}\right) + \left(\frac{E_a}{R}\right)\left(\frac{1}{T_p}\right) \tag{3}$$

Therefore, the activation energy E_a is estimated from the slope of the plot of $\ln\left(\frac{\beta}{T_p^2}\right)$ and $\left(\frac{1}{T_p}\right)$.

Figure 7 shows the Kissinger's activation energy plot for Al-Ni powder cryomilled for different milling times. It can be seen that the slope of the plot decreases with increasing milling time, which means that the activation energy has decreased as the milling progresses. For example, the activation energy of the powder milled for 1, 4 and 8 h are 84.72, 37.83, and 34.34 kJ/mol, respectively. It indicates that the difference in activation energy between the powder milled for 1 and 4 h is around two-fold (~46.89 kJ), while the activation energy obtained for 4 and 8 h is very small ~3.49 kJ/mol. As discussed in earlier sections, the difference in the reaction temperature between 1 and 4 h is larger as compared to that of between 4 and 8 h (about 68 °C). This means that the interface between the quasi-normal and the oxide-free zone has contributed to lowering the activation temperature by lowering the activation energy. The activation energy is lowest after 8 h of milling time due to the high number density of several repetitive bonded Al-Ni powder structures which are finer in size, so that the chance of reacting at low temperature is increased [24–26]. The activation energies calculated in the present study are significantly lower than those of other reports on high energy ball milling because of the minimization of reaction between Al and Ni powder during the cryogenic milling process [21,28].
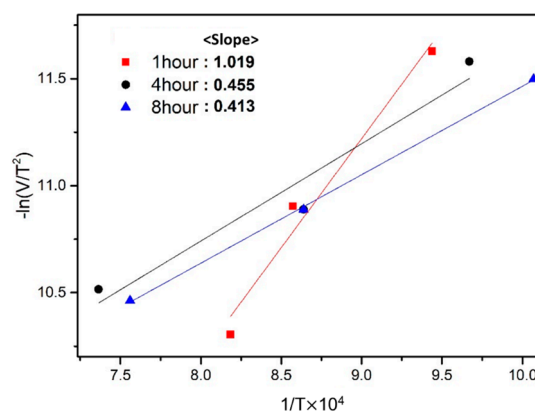

Figure 7. Activation energy plot generated by Kissinger analysis.

4. Conclusions

In this paper, a method of increasing the reactivity of Al-Ni mixed powder through cryomilling was studied. As the attrition milling process was carried out at the cryogenic temperature, it was found that the two materials (Al-Ni) were bonded to each other, almost similar to the conventional mechanical alloying but with a more homogeneous alloying free of Al-Ni reaction products. Thus, the reactive milling can be activated at a lower reaction temperature around 100 °C. The activation energy analysis shows that these two Al-Ni phases bond substantially and contribute to the reduction of the activation energy of Al-Ni reaction. The decrease in activation energy is thought to be due to the fact that Al and Ni bond to each other due to cryogenic milling to reduce the reaction distance and combine the two powders in a state in which no chemical reaction occurs with quasi-alloying of the bonding surface. Moreover, the destruction of the strong oxide during milling assists in lowering the activation energy significantly, although it was not observed in this experiment. If the subsequent cryogenic milling time is prolonged, Al and Ni powder particles are alternately arranged, and the metastable interface is formed of an Al-Ni powder having a repeated layered structure composed of a quasi-alloy phase free of oxides so that the reactivity can be further increased, as well as the reaction temperature can be lowered significantly.

Author Contributions: Minseok Oh and Min Chul Oh performed all materials processing, characterizations, and measurements. Sang-Hyun Jung and Byungmin Ahn formulated the idea. Minseok Oh and Byungmin Ahn wrote the manuscript. All co-authors participated in scientific discussion and manuscript preparation.

Conflicts of Interest: There is no conflict of interest to declare.

References

1. Adams, D.P. Reactive multilayers fabricated by vapor deposition: A critical review. *Thin Solid Films* **2015**, *576*, 98–128. [CrossRef]
2. Rogachev, A.S.; Mukasyan, A.S. Combustion of heterogeneous nanostructural systems (review). *Combust. Explos. Shock Waves* **2010**, *46*, 243–266. [CrossRef]
3. Floro, J.A. Propagation of explosive crystallization in thin Rh-Si multilayer films. *J. Vac. Sci. Technol.* **1986**, *4*, 631–637. [CrossRef]
4. Gavens, A.J.; Van Heerden, D.; Mann, A.B.; Reiss, M.E.; Weihs, T.P. Effect of intermixing on self-propagating reactions in Al/Ni nanolaminate foils. *J. Appl. Phys.* **2000**, *87*, 1255–1263. [CrossRef]
5. Mann, A.B.; Gavens, A.J.; Reiss, M.E.; Heerden, D.V.; Bao, G.; Weihs, T.P. Modeling and characterizing the propagation velocity of exothermic reactions in multilayer foils. *J. Appl. Phys.* **1997**, *82*, 1178–1188. [CrossRef]
6. Merzhanov, A.G.; Borovinskaya, I.P. Historical retrospective of SHS: An autoreview. *Int. J. Self-Propag. High-Temp. Synth.* **2008**, *17*, 242–265. [CrossRef]
7. Hilpert, K.; Kobertz, D.; Venugopal, V.; Miller, M.; Gerads, H.; Bremer, F.J.; Nickel, H. Phase diagram studies on the Al-Ni system. *Z. Naturforsch. A* **1987**, *42*, 1327–1332. [CrossRef]
8. Zhu, P.; Li, J.C.M.; Liu, C.T. Reaction mechanism of combustion synthesis of NiAl. *Mater. Sci. Eng. A* **2002**, *329–331*, 57–68. [CrossRef]
9. Mason, B.A.; Sippel, T.R.; Groven, L.J.; Gunduz, I.E.; Son, S.F. Combustion of mechanically activated Ni/Al reactive composites with microstructural refinement tailored using two-step milling. *Intermetallics* **2015**, *66*, 88–95. [CrossRef]
10. Mason, B.A.; Groven, L.J.; Son, S.F. The role of microstructure refinement on the impact ignition and combustion behavior of mechanically activated Ni/Al reactive composites. *J. Appl. Phys.* **2013**, *114*, 113501. [CrossRef]
11. Anselmi-Tamburini, U.; Munir, Z.A. The propagation of a solid-state combustion wave in Ni-Al foils. *J. Appl. Phys.* **1989**, *66*, 5039–5045. [CrossRef]

12. Hunt, E.M.; Granier, J.J.; Plantier, K.B.; Pantoya, M.L. Nickel aluminum superalloys created by the self-propagating high-temperature synthesis of nanoparticle reactants. *J. Mater. Res.* **2004**, *19*, 3028–3036. [CrossRef]

13. Gibbins, J.D.; Stover, A.K.; Krywopusk, N.M.; Woll, K.; Weihs, T.P. Properties of reactive Al: Ni compacts fabricated by radial forging of elemental and alloy powders. *Combust. Flame* **2015**, *162*, 4408–4416. [CrossRef]

14. Manukyan, K.V.; Tan, W.; Deboer, R.J.; Stech, E.J.; Aprahamian, A.; Wiescher, M.; Rouvimov, S.; Overdeep, K.R.; Shuck, C.E.; Weihs, T.P.; et al. Irradiation-enhanced reactivity of multilayer Al/Ni nanomaterials. *ACS Appl. Mater. Interfaces* **2015**, *7*, 11272–11279. [CrossRef] [PubMed]

15. Sraj, I.; Specht, P.E.; Thadhani, N.N.; Weihs, T.P.; Knio, O.M. Numerical simulation of shock initiation of Ni/Al multilayered composites. *J. Appl. Phys.* **2014**, *115*, 023515. [CrossRef]

16. Battezzati, L.; Pappalepore, P.; Durbiano, F.; Gallino, I. Solid state reactions in Al/Ni alternate foils induced by cold rolling and annealing. *Acta Mater.* **1999**, *47*, 1901–1914. [CrossRef]

17. Duckham, A.; Spey, S.J.; Wang, J.; Reiss, M.E.; Weihs, T.P.; Besnoin, E.; Knio, O.M. Reactive nanostructured foil used as a heat source for joining titanium. *J. Appl. Phys.* **2004**, *96*, 2336–2342. [CrossRef]

18. Noro, J.; Ramos, A.S.; Vieira, M.T. Intermetallic phase formation in nanometric Ni/Al multilayer thin films. *Intermetallics* **2008**, *16*, 1061–1065. [CrossRef]

19. Andrzejak, T.A.; Shafirovich, E.; Varma, A. Ignition mechanism of nickel-coated aluminum particles. *Combust. Flame* **2007**, *150*, 60–70. [CrossRef]

20. Simoes, S.; Viana, F.; Ramos, A.S.; Vieira, M.T.; Vieira, M.F. Anisothermal solid-state reactions of Ni/Al nanometric multilayers. *Intermetallics* **2011**, *19*, 350–356. [CrossRef]

21. Manukyan, K.V.; Mason, B.A.; Groven, L.J.; Lin, Y.C.; Cherukara, M.; Son, S.F.; Strachan, A.; Mukasyan, A.S. Tailored reactivity of Ni + Al nanocomposites: Microstructural correlations. *J. Phys. Chem. C* **2012**, *116*, 21027–21038. [CrossRef]

22. Blaine, R.L.; Kissinger, H.E. Homer Kissinger and the Kissinger equation. *Thermochim. Acta* **2012**, *540*, 1–6. [CrossRef]

23. Koch, C.C. Mechanical Milling and Alloying. In *Materials Science and Technology*; Cahn, R.W., Haasen, P., Kramer, E.J., Eds.; VCH Verlagsgesellschaft: Weinheim, Germany, 1991; Volume 15, pp. 193–246.

24. Koch, C.C. *Nanostructured Materials: Processing, Properties and Potential Applications*; William Andrew Publishing: Norwich, NY, USA, 2002.

25. White, J.D.; Reeves, R.V.; Son, S.F.; Mukasyan, A.S. Thermal explosion in Al-Ni system: Influence of mechanical activation. *J. Phys. Chem. A* **2009**, *113*, 13541–13547. [CrossRef] [PubMed]

26. Lagoviyer, O.S.; Schoenitz, M.; Dreizin, E.L. Effect of milling temperature on structure and reactivity of Al-Ni composites. *J. Mater. Sci.* **2018**, *53*, 1178–1190. [CrossRef]

27. Huang, B.L.; Vallone, J.; Luton, M.J. Formation of nanocrystalline B2 NiAl through cryomilling of Ni-50 at. % Al at 87 K. *Nanostruct. Mater.* **1995**, *5*, 411–424. [CrossRef]

28. Reeves, R.V.; Mukasyan, A.S.; Son, S.F. Thermal and impact reaction initiation in Ni/Al heterogeneous reactive systems. *J. Phys. Chem. C* **2010**, *114*, 14772–14780. [CrossRef]